An ALE Finite Element Method for Cohesionless Soil at Large Strains: Computational Aspects and Applications

Daniel Aubram, Frank Rackwitz & Stavros A. Savidis
Soil Mechanics and Geotechnical Engineering Division, Berlin Institute of Technology, Germany

ABSTRACT: The paper presents an arbitrary Lagrangian-Eulerian (ALE) finite element method for cohesionless soil to solve initial boundary value problems at large strains properly. It is based on an operator-split to simplify the needed algorithms, and to facilitate the upgrade of an existing finite element code. The solution then consists of a Lagrangian step, in which the mechanical behavior of the soil is modelled by a hypoplastic constitutive equation that describes the material state in terms of the stress, the void ratio, and a so-called intergranular strain. The following step applies an efficient optimization procedure to smooth the finite element mesh, and the final Eulerian step conservatively remaps the solution variables onto the updated mesh. Some numerical examples highlight the applicability of the ALE method, including benchmark tests for the algorithms, and simulation of pile penetration in sand.

1 INTRODUCTION

In soil mechanics and geotechnical engineering large strains may occur, for example, during pile installation, penetration of sounding tools, and slope failure. For these problems the classical Lagrangian and Eulerian finite element methods are often inapplicable. In the total and updated Lagrangian approaches generally applied to solid mechanics, the element mesh follows the material deformations so that solution may fail to proceed due to severe element distortion. Remeshing plus projection of the solution, also referred to as rezoning, is computationally expensive, and simple non-conservative projection methods based on interpolation introduce errors. Eulerian finite element approaches, which are generally applied by the computational fluid dynamics (CFD) community, keep the mesh fixed in space. This, however, makes the treatment of path dependent constitutive equations, free surfaces, and moving boundaries cumbersome.

The arbitrary Lagrangian-Eulerian (ALE) formulation (Hirt et al. 1974; Donea et al. 2004) has been developed to overcome the difficulties arising from the Lagrangian and Eulerian viewpoints, and to combine their advantages. ALE methods are nowadays standard for solving problems that involve large material deformations, e.g. industrial forming processes, simulation of crashworthiness, fluid-structure interaction, and free surface flow. Applications in computational soil mechanics are proposed quite recently (Di et al. 2007). The ALE finite element mesh is understood as an arbitrary moving reference domain that has a one-to-one correspondence with the initial configuration and the current configuration of the material body; differential geometry has been found to be the appropriate language to formulate this correspondence (Aubram 2009; Savidis et al. 2008). The physical motion of the body is described by a composition of two maps involving the reference domain. Instead of a complete remeshing applied in rezoned Lagrangian calculations, the ALE mesh is smoothed so that element distortion is reduced. The mesh topology is kept unchanged, and all elements have the same neighbors during the whole calculation. Therefore, CFD advection algorithms can be applied to project the solution onto the modified mesh in a conservative manner.

This paper presents an ALE method that we have implemented into a commercial finite element code in order to perform numerical simulations of pile installation in sand. An operator-split according to Benson (1989) has been applied to the basic ALE equations, so that a complex hypoplastic constitutive equation for sand (Niemunis and Herle 1997) can be incorporated in a pure Lagrangian step. The mechanical behavior of sand depends on the stress state and stress history, as well as on the density state. Therefore, density changes must be explicitly accounted for to satisfy conservation of mass with respect to the mov-

ing ALE mesh. To reduce element distortion, which plays a crucial role in the simulation of pile installation, mesh smoothing is carried out after the Lagrangian step. Because the explicit smoothing algorithms applied in several ALE methods are inapplicable to the non-convex mesh regions around the penetrated pile tip, we implemented an implicit optimization procedure that works quite well on structured and unstructured triangle meshes over arbitrarily shaped two-dimensional domains. After mesh smoothing, the solution variables are conservatively remapped onto the modified mesh along with the final Eulerian or advection step. A simple first-order accurate Godunov-like scheme (Rodríguez-Ferran et al. 1998) advects the element Jacobian, the stress, the void ratio of the sand, and the remaining history variables.

The structure of the paper is as follows. Section 2 derives the basic ALE equations, and section 3 briefly motivates the incorporation of a complex hypoplastic model for sand. Section 4 concerns computational aspects and the implementation into an existing finite element code. Applications of the ALE method are being presented in section 5, including benchmark tests for the algorithms, and recent simulation of pile penetration in sand. The paper closes with some concluding remarks.

2 BASIC ALE EQUATIONS

The section that follows should summarize the basic equations of the ALE framework. We apply a notation that is closely related to that of Marsden and Hughes (1994). For more details about the ALE formulation in continuum mechanics, see (Aubram 2009; Savidis et al. 2008), and the references already cited.

Let $\mathcal{I} \subset \mathbb{R}_+$ be a time interval and $t \in \mathcal{I}$, and let $\varphi_t : \mathcal{B} \to \mathcal{S}$, where $\varphi_t(\bullet) = \varphi(\bullet, t)$, be a motion of a material body $\mathcal{B}$ in the ambient space $\mathcal{S}$; usually one sets $\mathcal{S} = \mathbb{R}^3$, but this is an unnecessary limitation at the outset. We denote particles by $X \in \mathcal{B}$, and spatial points by $x \in \mathcal{S}$. Let the spatial (or Eulerian) velocity field of φ be $\boldsymbol{v}(x,t)$, with $x = \varphi(X,t)$, then the material (or Lagrangian) velocity is defined through the composition $\boldsymbol{V}_t(X) = (\boldsymbol{v}_t \circ \varphi_t)(X)$ at t fixed. More general, if a time-dependent tensor-valued field has the spatial resp. Eulerian description $f(x,t)$, then $F_t = f_t \circ \varphi_t$ is called its material resp. Lagrangian description, with $F_t(X) = F(X,t)$. The material time derivative of a field $f(x,t)$ on $\mathcal{S}$ is defined through

$$\dot{f}(x,t) = \left.\frac{\partial f}{\partial t}\right|_x (x,t) + (\boldsymbol{\nabla}_{\boldsymbol{v}} f)(x,t)\,, \tag{1}$$

where $x = \varphi(X,t)$. The term $\left.\frac{\partial f}{\partial t}\right|_x$ is the local or spatial time derivative, and $\boldsymbol{\nabla}_{\boldsymbol{v}} f$ is called the covariant derivative of f along $\boldsymbol{v}$.

The tangent $T\varphi = \boldsymbol{F}$ of the motion is called the deformation gradient. The spatial velocity gradient $\boldsymbol{\nabla}\boldsymbol{v} = \boldsymbol{d} + \boldsymbol{w}$ consists of the symmetric part $\boldsymbol{d}$, and the antisymmetric part $\boldsymbol{w}$, which are referred to as spatial rate of deformation and the spin, respectively. The volume elements $\mathbf{d}\boldsymbol{V}$ on $\mathcal{B}$, and $\mathbf{d}\boldsymbol{v}$ on $\mathcal{S}$ are related through $\varphi^\star \mathbf{d}\boldsymbol{v} = J\,\mathbf{d}\boldsymbol{V}$, where $\varphi^\star$ is the pullback operator concerning φ, and the evolution of the Jacobian J is specified by the equation

$$\dot{J} = (J \circ \varphi_t^{-1})\,\mathrm{tr}\,\boldsymbol{d}\,. \tag{2}$$

tr is the trace operator for second order tensors. Within the ALE formulation, an arbitrary moving subset $\mathcal{R} \subset \mathcal{S}$ is called a reference domain provided that there are diffeomorphisms $\Psi_t : \mathcal{R} \to \mathcal{B}$ and $\Phi_t : \mathcal{R} \to \varphi_t(\mathcal{B})$ such that

$$\varphi_t = \Phi_t \circ \Psi_t^{-1}\,. \tag{3}$$

The chain rule yields $\boldsymbol{F}_t = \boldsymbol{F}_{\Phi t} \cdot \boldsymbol{F}_{\Psi t}^{-1}$, where $\boldsymbol{F}_\Psi = T\Psi$, $\boldsymbol{F}_\Phi = T\Phi$, and $\cdot$ denotes the contraction of tensors. Moreover, let $\hat{\boldsymbol{v}}(x,t)$ be the spatial velocity of Φ_t, and $\boldsymbol{\vartheta}(\chi,t)$ the velocity of Ψ_t^{-1} at every reference point $\chi \in \mathcal{R}$, then

$$\boldsymbol{v}_t - \hat{\boldsymbol{v}}_t = \Phi_{t\star}\boldsymbol{\vartheta}_t\,. \tag{4}$$

The pushforward operator $\Phi_{t\star}$ concerning Φ_t has the explicit form $\Phi_{t\star}(\bullet) = (\boldsymbol{F}_{\Phi t} \cdot (\bullet)) \circ \Phi_t^{-1}$ for vector fields, and $\boldsymbol{c}_t = \Phi_{t\star}\boldsymbol{\vartheta}_t$ is called the convective velocity on $\mathcal{S}$, so $\boldsymbol{c}_t(x) = \boldsymbol{c}(x,t)$ is a spatial vector field. If one defines the referential description $\hat{f}(\chi,t)$ of a time-dependent field through its spatial description $f_t = \hat{f}_t \circ \Phi_t^{-1}$ resp. its material description $F_t = \hat{f}_t \circ \Psi_t^{-1}$, then (4) yields the fundamental ALE operator

$$\dot{f} = \left.\frac{\partial \hat{f}}{\partial t}\right|_\chi \circ \Phi^{-1} + \boldsymbol{\nabla}_{\boldsymbol{c}} f\,. \tag{5}$$

The arguments (x,t) have been suppressed. In order to obtain an ALE formulation of initial boundary value problems, one has to substitute the ALE operator for every material time derivative in the balance laws and the other basic equations that govern the problem. For example, (2) becomes

$$\left.\frac{\partial J}{\partial t}\right|_\chi + \boldsymbol{\nabla}_{\boldsymbol{c}} J = J\,\mathrm{tr}\,\boldsymbol{d}\,, \tag{6}$$

by dropping the point maps and arguments.

3 HYPOPLASTIC MODEL FOR SAND

The mechanical response of cohesionless soil resp. sand is very complex and has many influencing factors. One important characteristic that distinguishes sand from other materials is dilatancy, i.e. the

volume changes due to shear loading. Under monotonic shear loading, sand with a sufficiently low initial density contracts monotonically. If the initial density is sufficient high, sand shows little contraction at small shear strains, and then passes a transformation state at which the response changes from contractive to dilative. A similar behavior can be observed by varying the confining pressure instead of the initial density. Irrespective of the initial conditions, sand exhibits an isochoric response (zero dilatancy) at constant stress if shear deformation exceeds a specific value.

Dilatancy and the mechanical response of sand do not depend on the stress state and density state alone. Stress history due to monotonic or cyclic loading also plays a crucial role, as well as fabric anisotropy, saturation, and drainage conditions. Under cyclic loading and undrained conditions, the dilatancy of sand may lead to liquefaction because of a loss of shear resistance, or to cyclic mobility with limited shear deformation, dependent on the confining pressure, the loading amplitude, and the initial density. To reduce the amount of necessary concepts, however, in this paper we focus on dry sand, and assume isotropic response.

Although users can choose from a large amount of constitutive equations for soil, only a few simulate the mechanical behavior of sand at finite strains and under complex loading paths over a wide range of densities and stress states, by using only a single set of parameters. Aside fundamental discussion about the applicability of this approach, models based on the multiplicative split of the deformation gradient (Simo and Meschke 1993; Borja and Tamagnini 1995) require knowledge of the material deformation as a whole, which is —due to the non-Lagrangian view— usually unavailable in ALE regimes and thus would require additional data to be stored.

Nowadays standard for ALE computations are models of the rate-type, such as ad-hoc extensions of classical models of small-strain elasto-plasticity that generally apply a hypoelastic rate formulation of the stress response. While hypoelasticity assumes the relationship between an objective stress rate $\mathring{\boldsymbol{\sigma}}$ and the elastic rate of deformation $\boldsymbol{d}^{\text{el}} = \boldsymbol{d} - \boldsymbol{d}^{\text{pl}}$ to be linear (Truesdell and Noll 2004), the class of hypoplastic models developed by the "Karlsruher Schule" (Gudehus and Kolymbas 1979; Kolymbas 1991; von Wolffersdorff 1996; Niemunis and Herle 1997) include constitutive response functions that are non-linear in $\boldsymbol{d}$ and do not split deformation into elastic and plastic parts.

Into our ALE finite element method, we implemented the hypoplastic constitutive equation proposed by Niemunis and Herle (1997), which can be written in the form

$$\mathring{\boldsymbol{\sigma}}^{\text{ZJ}} = \boldsymbol{h}(\boldsymbol{\sigma}, e, \boldsymbol{\delta}, \boldsymbol{d})\,. \tag{7}$$

The state of sand is described by the Cauchy stress $\boldsymbol{\sigma}$, the void ratio e, and a so-called intergranular strain tensor $\boldsymbol{\delta}$ that covers low-cyclic loading effects (say $N_{\text{cycl}} < 10$). To obtain objective response, the Zaremba-Jaumann stress rate, $\mathring{\boldsymbol{\sigma}}^{\text{ZJ}} = \dot{\boldsymbol{\sigma}} + \boldsymbol{\sigma}\cdot\boldsymbol{w} - \boldsymbol{w}\cdot\boldsymbol{\sigma}$, has been chosen. The rate of e is obtained from the purely kinematic relation

$$\dot{e} = (1+e)\,\mathrm{tr}\,\boldsymbol{d}\,, \tag{8}$$

and the evolution of intergranular strain is described by a generally discontinuous response function for its objective rate $\mathring{\boldsymbol{\delta}}^{\text{ZJ}}$ (Niemunis and Herle 1997).

4 IMPLEMENTATION

In ALE finite element methods the mesh serves as the arbitrary moving reference domain introduced in section 2. We implemented a two-dimensional simple arbitrary Lagrangian-Eulerian (SALE) method according to (Benson 1989), which is restricted to a single material in each element, and material boundaries are resolved explicitly by element edges. An operator-split is applied to (5), yielding

$$\dot{f} = \Upsilon \qquad \text{and} \qquad \left.\frac{\partial f}{\partial t}\right|_{\chi} + \boldsymbol{\nabla}_{\boldsymbol{c}} f = 0\,, \tag{9}$$

by omitting the point maps and arguments from now on. Here Υ denotes a corresponding response function, e.g. a constitutive equation, and f is to be replaced by J, $\boldsymbol{\sigma}$, e, and $\boldsymbol{\delta}$, respectively. The Jacobian is included to update the element mass density consistent with mass conservation in every step according to $\rho = J^{-1}\rho_0$, where ρ_0 is the initial density. Note that in quasistatic analysis, balance of momentum remains unaffected by the ALE formulation (Donea et al. 2004).

Through the operator-split (Benson 1989), the needed algorithms are simpler and more robust than algorithms for the fully coupled problem. Another advantage growth from the facility to upgrade existing Lagrangian finite element codes; we have used ANSYS® as the background code. The solution proceeds in three steps. In the first step, $(9)_1$ is solved by means of standard updated Lagrangian methods for solid mechanics. To fulfill the objectivity requirement, recent ANSYS® versions apply a co-rotated formulation to rate-type constitutive equations (Hughes 1984). The hypoplastic model is integrated by a substepping algorithm with automatic error control. In the second step, mesh distortion is reduced by a smoothing procedure that does not change the topology of the mesh. The third step, called the Eulerian or advection step, is performed to solve $(9)_2$, i.e. to remap the solution onto the modified mesh with advection schemes proposed by the CFD community.

Time proceeds in the Lagrangian step, but it is fixed in the mesh smoothing and transport steps.

In a high quality mesh, no element becomes too large, and each element has low distortion. Mesh smoothing, therefore, plays a crucial role especially when non-convex regions are present, e.g. during pile penetration. The explicit smoothing algorithms applied in several ALE methods are often inapplicable. We implemented a robust implicit optimization scheme that works quite well on structured and unstructured triangle meshes over convex and non-convex domains. The objective function

$$W(\boldsymbol{x}^{\mathrm{v}}) = \sum_{\text{elements}} \frac{r_{\text{out}}}{r_0} \left(\frac{r_{\text{out}}}{r_{\text{in}}} \right)^3 = \text{Min.} \qquad (10)$$

has been chosen according to (Braess and Wriggers 2000). r_{out} denotes the circumcircle, and r_{in} the incircle of a triangle. $r_0 = 1.0$ is a reference radius. The sum is over the number of elements in the patch that enclose a single vertex node with position vector $\boldsymbol{x}^{\mathrm{v}}$. Therefore, the minimum of (10) is local. A global minimum is approximated by looping all the flagged vertex nodes intended for mesh smoothing.

To minimize the objective function W properly, we implemented a damped Newton's method with backtracking line search. Exact formulas for the gradient and Hessian of W are available. Armijo-Goldstein's rule is applied to decrease the step length if necessary, and the Goldstein-Price method is used to deal with non-positive definite Hessians (Sun and Yuan 2006).

Boundaries can be smoothed easily by averaging procedures in order to improve the quality of the complete mesh considerably (Aymone 2004). Corner nodes of the domain are not moved, because they shape the domain.

In the final advection step, the variables f calculated in the Lagrangian step are remapped onto the smoothed mesh, according to equation $(9)_2$. In $\mathbb{R}^3$, the convective velocity is given by

$$\boldsymbol{c} = \frac{\boldsymbol{x}_{\mathrm{L}} - \boldsymbol{x}_{n+1}}{\Delta t}\,, \qquad (11)$$

where $\boldsymbol{x}_{\mathrm{L}}$ and $\boldsymbol{x}_{n+1}$ are the nodal locations after the Lagrangian step and after the smoothing step, respectively. The convective velocity normal to the material boundaries is zero in SALE methods, because the same set of elements is associated with only one material during the whole calculation. For the solution of $(9)_2$, explicit advection algorithms are preferred. These are conditional stable provided that the material does not pass an element within one step (Courant-Friedrichs-Lewy condition), that is, if the load increments are not too large.

To avoid the evaluation of the gradient in $(9)_2$, a first-order accurate Godunov-like advection scheme (Rodríguez-Ferran et al. 1998) has been implemented. This technique assumes a piecewise constant field f, which is given directly when using constant strain triangles with a single Gauss point. For each triangle in plane conditions, the equation

$$f_{n+1} = f_{\mathrm{L}} - \frac{\Delta t}{2A} \sum_{i=1}^{3} \mathfrak{F}_{\mathcal{S}_i} (f^{\mathrm{c}}_{\mathcal{S}_i} - f_{\mathrm{L}})(1 - \operatorname{sgn} \mathfrak{F}_{\mathcal{S}_i}) \qquad (12)$$

has to be solved, in which f_{L} and f_{n+1} denote the values of f after the Lagrangian step and at the end of the load step, respectively, and $f^{\mathrm{c}}_{\mathcal{S}_i}$ is the value of f in the contiguous element owning the shared element edge $\mathcal{S}_i$. Moreover, A is the element area, sgn is the sign function, and $\mathfrak{F}_{\mathcal{S}_i} = \int_{\mathcal{S}_i} (\boldsymbol{n}^* \cdot \boldsymbol{c})\, \mathbf{d}\boldsymbol{S}$ is the volume flux across the element edge $\mathcal{S}_i$ with unit normal $\boldsymbol{n}^*$.

5 APPLICATIONS

A few numerical examples should highlight the applicability of our ALE algorithms to finite strain problems, particularly with regard to penetration of cohesionless soil.

The performance of the optimization scheme to smooth the two-dimensional triangle meshes used for the applications has been tested in several applications, including unstructured and structured meshes, as well as convex and non-convex regions. We have also implemented Guiliani's method (Giuliani 1982), and a simple averaging procedure (Aymone 2004) to compare different approaches.

Back extrusion is a common problem that involves large material strains and non-convex mesh regions. A rigid rough die is punched into a cylindrical workpiece with the vertical boundaries fixed in horizontal direction. The lower boundary is fixed in vertical direction. Figure 1 shows the edges of the undeformed workpiece, and the deformed mesh at different indentations. At 50% indentation, elements around the corner of the die are heavily squeezed when using Giuliani's method, which is shown on the left. The area of one element even vanishes (see detail in Fig. 1), which inhibits the convergence of the solution at higher indentations. The current mesh optimization scheme shown on the right keeps a good mesh quality. At 50% indentation, the squeeze and distortion of elements is moderate, even directly below the die. Calculation terminates not until indentation reaches a value of more than 71%. Only complete remeshing would eliminate element degeneration in order to ensure a convergent solution.

Figure 2 shows the results of a Molenkamp test (Molenkamp 1968) that has been carried out to test the advection algorithm. It is based on a purely Eulerian set up of the ALE method, which is obtained by fixing the mesh, i.e. $\boldsymbol{c} = \boldsymbol{v}$. The initial state of the virtual material is given by a distribution of a color

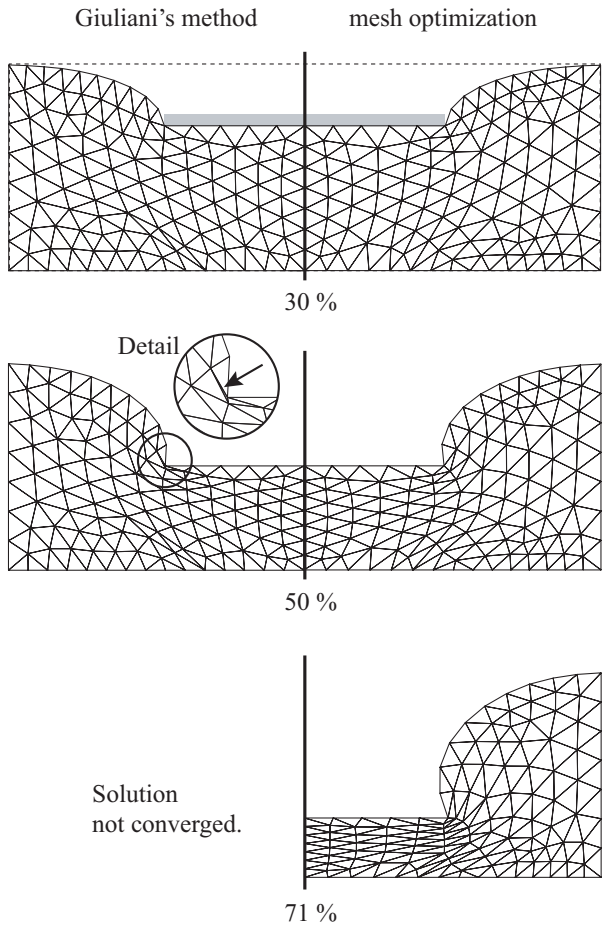

Figure 1: Comparison of Giuliani's method *(left)* and the current mesh optimization scheme *(right)* applied to back extrusion at different indentations.

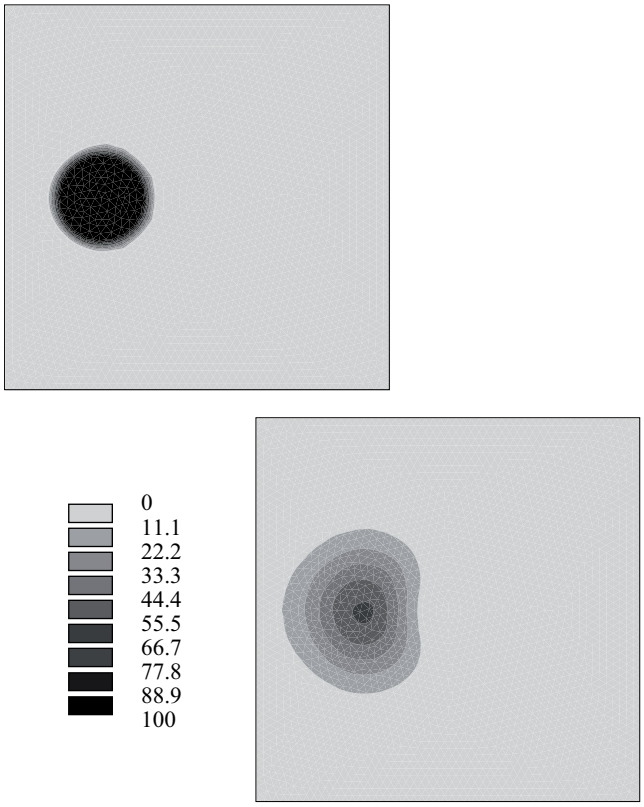

Figure 2: Molenkamp test of the advection algorithm. Initial distribution of the color function *(above)*, distribution after a full clockwise rotation (720 steps) of the material about the domain center *(below)*.

function shown in Figure 2 above. The initial state is assumed to be the solution obtained during the Lagrangian step of the operator-split ALE method, and the color function represents a variable that should be advected, that is, J, $\boldsymbol{\sigma}$, e, and $\boldsymbol{\delta}$ in our case. A spatial velocity field $\boldsymbol{v}$ is prescribed so that the material does a full 360° rigid clockwise rotation about the center of the square domain in 720 advection steps. The mesh used consists of 5516 triangle elements about the same size. The final state is shown in Figure 2 below.

It can be seen from Figure 2 that the implemented advection algorithm does transport material through the mesh in a Eulerian fashion. However, the initially circled area bounded by large gradients of the color function disperses, and the peak values are getting smeared as material rotation proceeds. This indicates the occurrence of high numerical diffusion, which results from the simplicity of the implemented first-order accurate Godunov-like algorithm. It has to be noted, however, that the Molenkamp test reflects an extreme example. The solution variables of realistic initial boundary value problems in soil mechanics often have smaller gradients, leading to less numerical diffusion. Moreover, in the operator-split ALE method, every advection step is followed by a Lagrangian step that brings back the solution variables to an admissible state. Therefore, the detail resolution of the material state variables, e.g. of the discontinuous intergranular strain, is predominantly determined by the coarseness of the mesh resp. the order of interpolation, and not by the advection algorithm.

Recent results of a quasistatic ALE pile penetration in sand are shown in Figure 3. The pile is assumed smooth and rigid, and the initial void ratio of the sand is set to $e_0 = 0.678$ ($D_{\mathrm{r0}} = 0.34$). As penetration starts from the soil surface, the initial configuration has a simple geometry. Contact elements are attached to the pile and soil surfaces, and a Lagrange multiplier contact algorithm enforces zero penetration of the pile elements when contact is closed. The number of axisymmetric solid elements used for the simulation is 35980, with the centerline of the pile serving as the axis of radial symmetry.

The deformed configuration and the void ratio distribution at a relative penetration depth of $d/D_{\mathrm{pile}} = 5.0$ shown in Figure 3 are reasonable. Since the pile displaces the soil, soil heaving occurs lateral to the pile. Along with the pile shaft the initially medium-dense sand loosens, while densification arises below the pile tip. It is worth mentioning that numerical simulation of pile penetration in sand is hard to challenge. Loading has to be increased very slowly, and adjust-

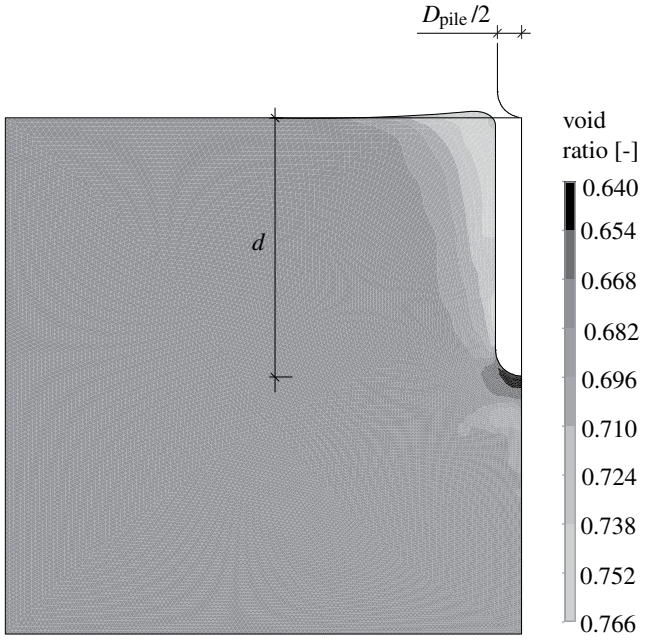

Figure 3: Penetration of a smooth rigid pile into sand (initial void ratio $e_0 = 0.678$ ($D_\text{r} = 0.34$)). Edges of the undeformed configuration, and void ratio distribution at a relative penetration depth of $d/D_{\text{pile}} = 5.0$.

ing the contact parameters at the beginning of the simulation only is a science of its own.

6 CONCLUSIONS

An ALE finite element method for sand at large strains has been presented. The split of the ALE operator simplifies the incorporation of a complex hypoplastic model for sand in a pure Lagrangian step, and facilitates the upgrade of existing FE codes. For the mesh smoothing step, an efficient and robust optimization scheme has been proposed, and the final advection step applies a simple Godunov-like algorithm. Numerical examples demonstrate the applicability of the ALE method, particularly to pile penetration in sand.

7 ACKNOWLEDGEMENTS

We would like to acknowledge the financial support to carry out our presented research work, which has been provided by the DFG (German Research Foundation), grant SA 310/21-2.

REFERENCES

Aubram, D. (2009). *Differential Geometry Applied to Continuum Mechanics*, Volume 44 of *Veröffentlichungen des Grundbauinstitutes der Technischen Universität Berlin*. Shaker Verlag GmbH, Aachen, Germany. (Institute Series).

Aymone, J. L. F. (2004). Mesh motion techniques for the ale formulation in 3d large deformation problems. *International Journal for Numerical Methods in Engineering 59*, 1879–1908.

Benson, D. J. (1989). An efficient, accurate, simple ale method for nonlinear finite element programs. *Computer Methods in Applied Mechanics and Engineering 72*(3), 305–350.

Borja, R. I. and C. Tamagnini (1995). Finite deformation theory for a cam-clay model. In G. N. Pande and S. Pietruszczak (Eds.), *Numerical Models in Geomechanics - NUMOG V*, pp. 3–8. Balkema.

Braess, H. and P. Wriggers (2000). Arbitrary lagrangian eulerian finite element analysis of free surface flow. *Computer Methods in Applied Mechanics and Engineering 190*, 95–109.

Di, Y., J. Yang, and T. Sato (2007). An operator-split ale model for large deformation analysis of geomaterials. *International Journal for Numerical and Analytical Methods in Geomechanics 31*, 1375–1399.

Donea, J., A. Huerta, J.-P. Ponthot, and A. Rodríguez-Ferran (2004). *Arbitrary Lagrangian-Eulerian Methods*, Volume 1 of *Encyclopedia of Computational Mechanics*, Chapter 14. John Wiley & Sons, Ltd.

Giuliani, S. (1982). An algorithm for continuous rezoning of the hydrodynamic grid in arbitrary lagrangian-eulerian computer codes. *Nuclear Engineering and Design 72*, 205–212.

Gudehus, G. and D. Kolymbas (1979). A constitutive law of the rate type for soils. In W. Wittke (Ed.), *Proceedings Third International Conference on Numerical Methods in Geomechanics, Aachen, Germany*, pp. 319–329. A. A. Balkema.

Hirt, C. W., A. A. Amsden, and J. L. Cook (1974). An arbitrary lagrangian-eulerian computing method for all flow speeds. *Journal of Computational Physics 14*, 227–253.

Hughes, T. J. R. (1984). Numerical implementation of constitutive models: rate-independent deviatoric plasticity. In S. Nemat-Nasser, R. J. Asaro, and G. A. Hegemier (Eds.), *Theoretical Foundation for Large-Scale Computations for Nonlinear Material Behavior*, pp. 29–63. Martinus Nijhoff Publishers, Dordrecht, Niederlande.

Kolymbas, D. (1991). An outline of hypoplasticity. *Archive of Applied Mechanics 61*(3), 143–151.

Marsden, J. E. and T. J. R. Hughes (1994). *Mathematical Foundations of Elasticity*. Dover Publications, New York. (Originally published: Prentice-Hall, 1983).

Molenkamp, C. R. (1968). Accuracy of finite-difference methods applied to the advection

equation. *Journal of Applied Meteorology 7*, 160–167.

Niemunis, A. and I. Herle (1997). Hypoplastic model for cohesionless soils with elastic strain range. *Mechanics of Cohesive-Frictional Materials 2*, 279–299.

Rodríguez-Ferran, A., F. Casadei, and A. Huerta (1998). Ale stress update for transient and quasistatic processes. *International Journal for Numerical Methods in Engineering 43*, 241–262.

Savidis, S. A., D. Aubram, and F. Rackwitz (2008). Arbitrary lagrangian-eulerian finite element formulation for geotechnical construction processes. *Journal of Theoretical and Applied Mechanics 38*(1-2), 165–194.

Simo, J. C. and G. Meschke (1993). A new class of algorithms for classical plasticity extended to finite strains. application to geomaterials. *Computational Mechanics 11*, 253–278.

Sun, W. and Y. Yuan (2006). *Optimization Theory and Methods - Nonlinear Programming*. Springer Science+Business Media, LLC.

Truesdell, C. and W. Noll (2004). *The Non-Linear Field Theories of Mechanics* (3rd ed.). Springer-Verlag Berlin Heidelberg New York.

von Wolffersdorff, P.-A. (1996). A hypoplastic relation for granular materials with a predefined limit state surface. *Mechanics of Cohesive-Frictional Materials 1*, 251–271.